International Journal of Academic Multidisciplinary Research (IJAMR)
ISSN: 2643-9670
Vol. 10 Issue 6 June - 2026, Pages: 1-10

Quantifying Green Infrastructure Resilience In Arid Urban Systems: Methodological Advances Combining Mspa, Mcr, And Conefor

Mamirova Zulfiyaxon Ibroximjon qizi

"PhD Student at Fergana State University

mamirovazulfiya3@gmail.com

ORCID: 0009-0000-6283-7496

Abstract: *Green infrastructure (GI) sustains the ecological processes, thermal moderation, and habitability of urban areas, but across arid and semi-arid cities it remains thinly distributed, severely fragmented, and especially vulnerable to water shortages and heat extremes. Gauging the resilience of these networks—that is, their ability to preserve connectivity and function when disturbed—calls for approaches that simultaneously describe spatial configuration, the potential for movement, and the systemic weight of individual elements. The present study formulates and illustrates an integrated methodological framework in which Morphological Spatial Pattern Analysis (MSPA), Minimum Cumulative Resistance (MCR) corridor modelling, and graph-theoretic connectivity analysis in Conefor are combined to measure GI resilience in dryland settings. MSPA divides the GI mask into structurally and functionally distinct classes; MCR traces least-cost corridors over a land-cover resistance surface; and Conefor orders patches and links by how much they add to overall connectivity, using the Integral Index of Connectivity and the Probability of Connectivity. Resilience is made operational through redundancy, the retention of connectivity, and robustness against simulated disturbance, encompassing the targeted removal of nodes and links as well as drought-induced rises in matrix resistance. Drawing on a representative arid-city configuration, we show how this joint procedure pinpoints pivotal hubs, stepping-stone patches, and corridor bottlenecks that analyses based on a single method tend to miss. The framework produces spatially explicit and reproducible resilience priorities capable of guiding water-efficient GI planning, the safeguarding of corridors, and restoration in dryland cities. We close by considering the methodological contributions, the mutual validation among the indices, the principal limitations, and avenues for empirical testing.*

Keywords: green infrastructure; landscape connectivity; ecological resilience; arid cities; morphological spatial pattern analysis; minimum cumulative resistance; Conefor; graph theory

1. INTRODUCTION

Urban green infrastructure (GI)—the linked system of parks, street trees, vegetated corridors, wetlands, and further semi-natural features—has moved to the heart of agendas for sustainable and liveable cities (Benedict & McMahon, 2006; Tzoulas et al., 2007). In addition to furnishing habitat, GI tempers microclimate, buffers stormwater, stores carbon, and bolsters human well-being, and its worth is more and more expressed through the resilience it lends to urban social–ecological systems (Folke, 2006; Meerow et al., 2016). In the ecological sense first articulated by Holling (1973), resilience refers to a system's ability to absorb disturbance and reorganise while still preserving broadly the same function, structure, and feedbacks (Walker et al., 2004). For GI, one decisive ingredient of that ability is connectivity—the extent to which the network enables ecological flows of organisms, propagules, water, and genes across the urban matrix (Taylor et al., 1993; Forman, 1995).

Such functions come under acute pressure in arid and semi-arid cities. Drylands are characterised by scarce and erratic rainfall, elevated potential evapotranspiration, and repeated water shortfalls, with the consequence that urban vegetation tends to be sparse, spatially concentrated around irrigated zones, and sustained only at substantial expense (Pickett et al., 2001; Grimm et al., 2008). Swift urban growth, rival claims on limited water, sharpening heat extremes, and soil salinisation together worsen the fragmentation of an already restricted stock of green space. What emerges is a GI network that is structurally meagre and unduly reliant on a handful of patches and connections—a situation in which losing even a few elements can precipitate steep drops in connectivity. Measuring and protecting the resilience of dryland GI is thus an urgent planning concern, and yet one in which structurally sparse, water-constrained networks are ill served by methods tuned to temperate, vegetation-rich landscapes.

Landscape ecology supplies a well-developed set of tools for examining connectivity, although the pertinent methods tackle distinct and only partly overlapping aspects of the question. Structural connectivity—the physical arrangement and contiguity of habitat—can be described through Morphological Spatial Pattern Analysis (MSPA), which runs mathematical-morphology operators over a binary habitat mask and sorts it into mutually exclusive categories: core, islet, perforation, edge, loop, bridge, and branch (Soille & Vogt, 2009; Vogt et al., 2007). MSPA is computationally light and requires few parameters, and it has served to map and track GI from regional up to national scales (Wickham et al., 2010). It nonetheless captures pattern rather than process and takes no account of how permeable the surrounding matrix is.

Functional connectivity—how the matrix shapes movement—is most often represented with the Minimum Cumulative Resistance (MCR) method, whereby every land-cover type receives a resistance (cost) value and least-cost routes or cumulative-cost surfaces are derived from source patches (Knaapen et al., 1992; Adriaensen et al., 2003). MCR forms the basis of the much-used ecological security pattern framework in planning (Yu, 1996) and delivers explicit corridors and pinch points, even though its results are sensitive to the resistance values adopted and to the premise of optimal, cost-minimising movement. Circuit-theoretic approaches loosen that premise by depicting numerous pathways at once (McRae et al., 2008), yet they likewise hinge on how resistance is parameterised.

The systemic importance of individual elements—the amount that each patch or link adds to the connectivity of the entire network—is best captured by the graph-theoretic indices built into Conefor. Pascual-Hortal and Saura (2006) and Saura and Pascual-Hortal (2007) put forward habitat-availability indices, chiefly the Integral Index of Connectivity (IIC) and the Probability of Connectivity (PC), together with the companion importance measures dIIC and dPC, which order elements according to the connectivity forfeited when they are removed (Saura & Torné, 2009). Breaking dPC down into its intra-patch, flux, and connector fractions additionally separates large habitat hubs from small yet strategically placed stepping stones (Saura & Rubio, 2010). Graph-based methods scale well and have been rendered operational for spatial planning (Kong et al., 2010; Zetterberg et al., 2010), but in isolation they set aside the morphological structure and matrix resistance that MSPA and MCR encode.

Each method therefore addresses a necessary but on its own inadequate facet of resilience: MSPA the network's structural redundancy, MCR its movement potential and bottlenecks, and Conefor the systemic importance and contribution of its constituent parts. In practice these instruments are usually deployed separately, or at best as loosely linked pairs, and the assessments they produce seldom examine how the network responds to disturbance. This is an especially serious gap for arid cities, where sparse cores, few bridges, and high matrix resistance cause structure, movement, and importance to interact in ways that no individual index exposes, and where spells of drought and heat operate as recurring, spatially widespread disturbances. What is needed, then, is an integrated and disturbance-aware framework that brings together all three method families and converts their outputs into explicit indicators of redundancy and robustness.

The present study builds and demonstrates exactly such a framework. Its particular aims are: (i) to set out a workflow that links MSPA, MCR, and Conefor so that their outputs reinforce one another instead of duplicating information; (ii) to render GI resilience operational by means of complementary indicators of structural redundancy, connectivity, and robustness under simulated disturbance; (iii) to specify a transparent composite element-importance score that cross-checks priorities across the three methods; and (iv) to show, with a representative arid-city configuration, how the integrated approach detects key hubs, stepping stones, and corridor bottlenecks that single-method analyses miss, and to consider what this implies for water-efficient GI planning. The contribution is methodological: rather than presenting a validated empirical assessment of a particular city, we offer a reproducible procedure and an illustrative demonstration meant to be parameterised with local data.

2. MATERIALS AND METHODS

2.1. Conceptual framework and the operationalisation of resilience

We represent the GI of a dryland city as a spatial graph whose nodes are habitat patches and whose links are functional connections governed by the matrix. After Holling (1973) and Walker et al. (2004), we separate resilience into three measurable attributes of this graph. Structural redundancy denotes the presence of several partially interchangeable structural elements—cores and the bridges linking them—so that the network does not rest entirely on any one component; this is obtained from MSPA. Connectivity denotes the realised scope for ecological flow across the matrix and is captured together by MCR corridors and Conefor availability indices. Robustness, and its corollary the ability to recover, denotes the extent to which connectivity persists as elements are lost or matrix resistance climbs, and is gauged by exposing the graph to disturbance scenarios. Figure 1 outlines the workflow: inputs pass through MSPA, MCR, and Conefor in sequence, each supplying a separate facet, and their outputs are merged into a composite assessment that is subsequently stress-tested.

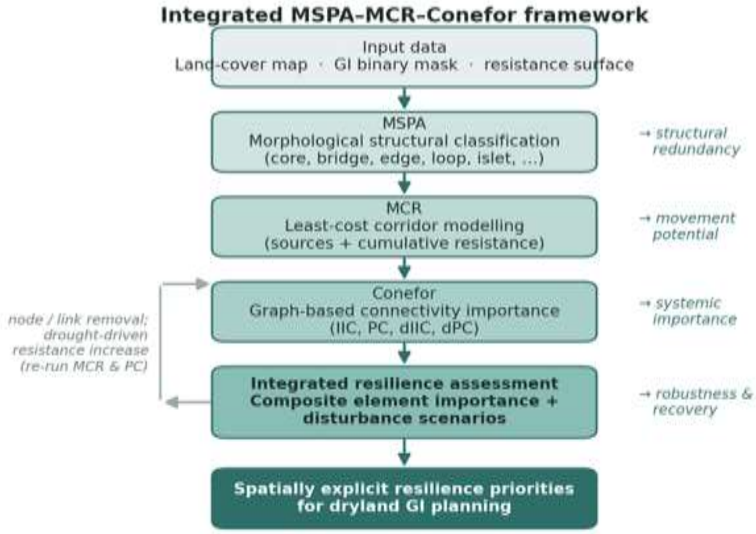

Figure 1. The integrated methodological workflow. Every analytical stage supplies a separate dimension of resilience, and the disturbance scenarios (left) loop back into the corridor and connectivity steps to probe robustness.

2.2. Demonstration context and input data

To give the workflow concrete form, we apply it to a representative arid urban landscape—a mid-sized city situated on a semi-arid plain, where irrigated green space gathers along watercourses and in formal parks and is encircled by a thinly vegetated matrix of built-up land and bare soil. Such a configuration is characteristic of numerous cities across Central Asia, the Middle East, North Africa, and the south-western United States. We stress that the data employed here are illustrative: the land-cover categories, patch geometry, and parameter values are selected to exercise the method and to display the form of its outputs, not to convey empirical results for any named city. In an applied investigation, the identical workflow would be fed with classified satellite imagery (from Sentinel-2 or Landsat, for instance), a locally validated land-cover map, and resistance values calibrated against target taxa or expert judgement. Three inputs are required: a categorical land-cover map; a binary GI mask derived from it, in which vegetated and permeable features form the foreground and everything else the background; and a resistance surface that attaches a movement cost to each land-cover class.

2.3. Morphological Spatial Pattern Analysis

MSPA was run on the binary GI mask through the chain of morphological operators provided in the GuidosToolbox (Soille & Vogt, 2009; Vogt et al., 2007). Foreground (GI) pixels were processed under eight-neighbour connectivity, and an edge width of a single pixel set the transition zone between core and surroundings; this parameter governs the thickness of the edge and perforation classes and is chosen to align with the spatial resolution of the input. The routine divides the foreground into seven mutually exclusive classes—core, islet, perforation, edge, loop, bridge, and branch—each carrying a separate meaning for connectivity (Table 1). For the resilience assessment the two most informative classes are core, standing for interior habitat able to function as a source, and bridge, standing for foreground that joins two or more distinct cores and so forms a structural corridor. Islets (isolated fragments) and branches (elements attached at only one end) indicate a network dependent on small or dead-ended pieces, a signature of fragmented dryland GI.

MSPA class	Structural meaning	Role in network resilience
Core	Interior foreground beyond the edge width; the largest contiguous habitat	Primary sources/hubs; loss removes habitat and anchor nodes
Islet	Isolated foreground too small to contain core	Fragments; contribute little unless they act as stepping stones

MSPA class	Structural meaning	Role in network resilience
Perforation	Internal boundary around gaps within core	Indicates internal fragmentation and edge exposure of cores
Edge	Outer boundary of core areas	High perimeter-to-area ratio; sensitive to heat and desiccation
Loop	Connector joining the same core back to itself	Provides alternative within-patch routes; modest redundancy
Bridge	Connector joining two or more different cores	Structural corridors; scarcity signals low structural redundancy
Branch	Connected to the network at one end only	Dead-ended elements; do not relay flow between cores

Table 1. The Morphological Spatial Pattern Analysis (MSPA) classes and how each is interpreted for green-infrastructure resilience.

2.4. Source patches and the resistance surface

Core areas above a minimum size threshold were kept as source patches (nodes) for the corridor and connectivity analyses that follow, so that the graph is grounded in functionally meaningful habitat rather than in incidental pixels. Every land-cover class was then given a resistance value on a relative scale, with permeable, vegetated covers receiving low resistance and impervious, hostile, or barrier covers receiving high resistance (Table 2). Resistance values represent the most influential and least certain decision in the workflow; we accordingly treat them as explicit assumptions open to calibration and, within the disturbance analysis (Section 2.7), intentionally perturb them to emulate drought.

Land-cover class	Resistance	Rationale
Dense vegetation / woodland	1	Most permeable; preferred movement habitat
Parks and managed green space	5	Permeable but with human disturbance
Riparian / wetland corridor	3	Permeable linear habitat aligned with watercourses
Irrigated agriculture / gardens	20	Seasonally permeable; moderate cost
Bare soil / sparse steppe	50	Exposed, low-cover matrix typical of drylands
Low-density built-up	150	Partly permeable urban fabric
High-density built-up / sealed	500	Hostile, largely impermeable matrix
Major roads / infrastructure	1000	Near-absolute movement barriers

Table 2. Illustrative relative resistance values given to land-cover classes in the Minimum Cumulative Resistance model. The values are demonstrative and would be calibrated to local conditions in an applied study.

2.5. Minimum Cumulative Resistance corridor modelling

For each source patch a cumulative-resistance surface was produced by summing the cost of crossing the resistance surface outward over the landscape (Knaapen et al., 1992; Adriaensen et al., 2003). Least-cost routes between adjacent sources define candidate corridors, while the lower envelope of the cumulative-cost surfaces marks out corridor swaths within which movement encounters the least impedance. Places where a corridor contracts because high-resistance land cover restricts the available route—pinch points or bottlenecks—were located as the cells whose removal would most enlarge least-cost distances; these are structurally critical since few or no alternative routes are available. The MCR analysis therefore supplies both the corridor geometry that ties the graph together and an initial signal of where that linkage is weak. In keeping with the ecological-security-pattern logic (Yu, 1996), corridors and pinch points were taken forward as candidate links and as priority locations for protection.

2.6. Graph-based connectivity analysis in Conefor

The node set (source patches) and the inter-patch distances—treated as effective, cost-weighted distances obtained from the MCR surface in place of straight-line distances—were brought into Conefor (Saura & Torné, 2009). Two habitat-availability indices were calculated. The Integral Index of Connectivity (IIC) rests on a binary connection model and topological path lengths, whereas the Probability of Connectivity (PC) rests on a probabilistic connection model in which the chance of direct movement between two patches decreases with distance (Pascual-Hortal & Saura, 2006; Saura & Pascual-Hortal, 2007). A median dispersal distance—the distance at which the connection probability takes a reference value—was set to correspond to a generic, moderately mobile organism, and patch area acted as the node attribute. The importance of each element was expressed as the percentage drop in the index produced by its removal (dIIC, dPC). Importantly, dPC was split into its intra, flux, and connector fractions (Saura & Rubio, 2010): a large intra or flux fraction marks extensive, well-connected habitat hubs, while a large connector fraction marks stepping-stone patches whose main worth is to relay flow among other patches—exactly the elements that supply redundancy in sparse networks. Table 3 sets out the indices applied.

Index	Description	What it captures
IIC	Integral Index of Connectivity; binary connection model using topological distances between patches	Topological habitat availability; robust where distances are coarse
PC	Probability of Connectivity; probabilistic model with dispersal probability declining with distance	Distance-weighted habitat availability; sensitive to dispersal range
dPC	Percentage decrease in PC when an element is removed	Overall importance of a patch or link for connectivity
dPC fractions	Decomposition of dPC into intra, flux, and connector components	Distinguishes habitat hubs (intra/flux) from stepping stones (connector)

Table 3. The graph-theoretic connectivity indices calculated in Conefor and the property that each one captures.

2.7. Integrated resilience indicators and disturbance scenarios

The three streams were merged in two ways. First, a composite element-importance score was derived for every patch by min–max rescaling three inputs to the 0–1 range and combining them through weights: a structural weight from MSPA (with cores and bridge-adjacent patches scoring highest), a corridor weight from MCR (with patches lying within or terminating high-traffic, bottleneck-prone corridors scoring highest), and a connectivity weight from Conefor (the normalised dPC). Equal weights were adopted in the demonstration, and how sensitive the ranking is to the weighting scheme is taken up in Section 4. The composite makes plain where the three methods concur—high-confidence priorities—and where they part company, as with a patch that is structurally unremarkable yet shows a high connector-fraction dPC.

Second, resilience was measured by exposing the graph to two families of disturbance and following the response of PC, stated relative to its undisturbed value. Under targeted and random element loss, nodes and links were deleted one after another, either in descending order of composite importance (targeted) or in random order averaged across repeated draws, and the resulting connectivity-retention curve was logged. The area beneath the targeted-removal curve, and how far it departs from the random curve, summarise the degree to which connectivity is concentrated in a few elements: the greater the concentration, the lower the structural resilience. In the drought-driven resistance scenario, matrix resistance values were increased by a fixed multiplier to reproduce the diminished permeability and vegetation stress of a drought episode, the MCR surface and effective distances were recalculated, and the fall in PC was logged. A redundancy index, built from the availability of alternative near-least-cost routes between source pairs, supplemented these measures. Figure 2 depicts the anticipated shape of the retention curves and the resilience gain attributable to protecting the priority elements that the framework identifies.

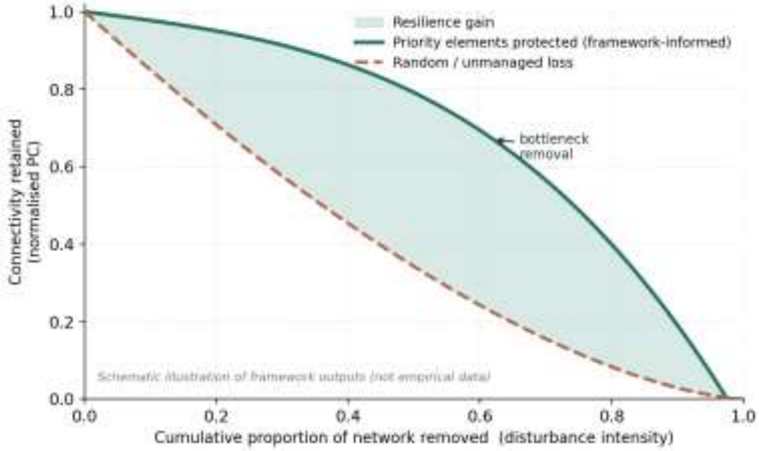

Figure 2. Schematic connectivity-retention curves as disturbance intensifies. Safeguarding the priority elements identified by the framework (solid) preserves more connectivity than unmanaged loss (dashed); the shaded region marks the resilience gain. The curves illustrate the form of the method's outputs and are not empirical data.

2.8. Software and reproducibility

MSPA was carried out in the GuidosToolbox; the resistance surface, cumulative-cost modelling, and the extraction of corridors and pinch points were handled with standard least-cost tools within a geographic information system; and the connectivity indices were obtained in Conefor 2.6 (Saura & Torné, 2009). Every parameter—edge width, source-size threshold, resistance values, dispersal distance, composite weights, and disturbance multipliers—is reported so that the workflow can be replicated and re-parameterised with local data. Since each step relies on openly specified inputs and freely accessible software, the procedure transfers readily across dryland cities.

3. RESULTS

3.1. Morphological structure

MSPA yielded a foreground governed by peripheral and linear classes rather than interior habitat—the structural hallmark of a sparse, fragmented dryland network. In the demonstration, core made up about two-fifths of the GI area but was confined to a few large irrigated parks and riparian strips; edge and perforation jointly accounted for a considerable proportion, in line with the high perimeter-to-area ratio of narrow, irrigation-dependent vegetation; and islets and branches—isolated fragments and dead-ended elements—were plentiful though small individually. Bridges, the structural connectors that link separate cores, were relatively few and spatially clustered, so that the network's contiguity depended on comparatively few morphological links. This makeup points to limited structural redundancy: with few bridges and cores, the network has scant ability to absorb the loss of any one connector.

3.2. Corridor network

The MCR model connected the source patches into a branching corridor network arranged around the main watercourse and the largest parks, which served as origins for several least-cost routes. A number of corridors were channelled through narrow openings in the built matrix, generating well-defined pinch points at which the least-cost route had no close alternative; in these places a slight loss of permeable land cover markedly raised the effective distances between patches that were otherwise well connected. The corridor geometry bore out the MSPA inference that linkage within the network was sustained by a limited set of elements, and it pinpointed that fragility to specific, mappable bottlenecks amenable to targeted intervention.

3.3. Connectivity importance

Conefor ordered the source patches by dPC and exposed a steep importance gradient: a handful of patches contributed disproportionately to overall connectivity, whereas most made only minor individual contributions. Decomposing dPC explained the reason. The top-ranked patches were large parks and riparian cores with high intra and flux fractions—habitat hubs whose worth lay in their own extent and in their strong links to neighbours. A second and distinct group ranked highly mainly through the connector fraction: these were small or medium patches sited between hubs, serving as stepping stones whose removal would cut or extend indirect pathways. The IIC and PC rankings coincided closely for the leading hubs but parted for several mid-ranked patches, the probabilistic PC assigning more weight to stepping stones at intermediate distances—a telling distinction for sparse networks in which indirect connectivity is consequential.

International Journal of Academic Multidisciplinary Research (IJAMR)
ISSN: 2643-9670
Vol. 10 Issue 6 June - 2026, Pages: 1-10

3.4. Integrated resilience assessment

The composite score drew these threads together. A central set of elements scored highly under all three methods—large riparian cores that are at once MSPA cores, MCR corridor origins, and high-dPC hubs—forming clear, high-confidence priorities for protection. Just as important, the integration brought to light elements that no single method would have flagged confidently: stepping-stone patches that were structurally unremarkable (small, frequently classed as islet or branch) and modest in area individually, yet bore a high connector-fraction dPC and overlapped with MCR pinch points. These divergence cases are the redundancy-bearing elements of the network, and treating them as priorities is the principal practical reward of the combined approach.

The disturbance analysis put a number on the network's fragility. Under targeted removal in descending order of composite importance, connectivity (PC) fell sharply once only a few elements had been lost, and the area beneath the targeted-removal retention curve was considerably smaller than under random removal—a diagnostic of a network in which connectivity is concentrated in few components and structural redundancy is low. The drought scenario, applied as a uniform rise in matrix resistance, brought about a further, system-wide decline in PC and stretched effective distances most acutely along the pinch-point corridors identified by the MCR model, confirming that the same elements are critical under both element-loss and matrix-stress disturbances. By contrast, the schematic retention curves in Figure 2 indicate that protecting the small set of framework-identified priority elements—hubs together with the highest connector-fraction stepping stones—preserves appreciably more connectivity across the disturbance gradient than unmanaged loss, the shaded area standing for the resilience gain that targeted protection delivers. Table 4 lists representative top-ranked elements alongside their MSPA class, corridor role, dPC, composite score, and sensitivity under the disturbance scenarios.

Element	MSPA class	Corridor role	dPC (%)	Composite	Sensitivity
P-01	Core	Corridor origin (hub)	24.6	0.97	High
P-02	Core	Corridor origin (hub)	18.1	0.89	High
P-07	Bridge	Pinch-point link	9.4	0.81	Critical
P-12	Islet	Stepping stone	7.8	0.74	Critical
P-05	Core	Hub	11.2	0.71	Medium
P-18	Branch	Stepping stone	5.3	0.63	High
P-23	Islet	Stepping stone	3.9	0.55	Medium

Table 4. Representative top-ranked green-infrastructure elements yielded by the integrated assessment (illustrative). Composite scores are normalised to 0–1; the sensitivity flag identifies the elements whose loss most reduces connectivity under the disturbance scenarios

4. DISCUSSION

4.1. The value of integration

The chief methodological advance of this study is to demonstrate that MSPA, MCR, and Conefor are complementary rather than interchangeable, and that uniting them produces a fuller and more decision-relevant portrait of GI resilience than any one of them in isolation. Each method answers a different question—what the network looks like, how movement passes through it, and which parts count most—and the value of the integration lies precisely in how their answers relate to one another. Where the three agree, they cross-validate one another and pick out priorities in which planners can place high confidence. Where they disagree, the discrepancy is itself informative: the recurrent case of a structurally minor patch carrying a high connector-fraction dPC at an MCR pinch point would be overlooked by a structural analysis, undervalued by an area-based screen, and only faintly flagged by any single connectivity index, yet it is exactly the sort of stepping stone whose protection lends redundancy to a sparse network. Triangulation across methods therefore accomplishes what no single, more intricate method can: it distinguishes robust priorities from artefacts peculiar to one method.

4.2. Resilience operationalisation and arid specificity

A second advance is the explicit, disturbance-aware way in which resilience is made operational. Instead of treating resilience as a static connectivity score, we assess it through redundancy—the availability of substitutable elements and alternative routes—and through robustness, the connectivity that survives element loss and matrix stress. This is of particular consequence in drylands. The demonstration recreated the typical structural signature of arid GI, with plentiful edge and branch and scarce core and bridge, and showed how that signature gives rise to low structural redundancy and steep connectivity loss under targeted disturbance. The drought scenario further laid bare a vulnerability peculiar to water-limited systems: because dryland GI relies on irrigation and on a permeable matrix that itself deteriorates under water stress, a widespread rise in resistance wears away connectivity throughout the system and focuses its effect on precisely the corridors that the MCR model flags as bottlenecks. Methods tuned to vegetation-rich temperate landscapes, where cores are extensive and matrices comparatively benign, may understate these effects; incorporating a resistance-perturbation scenario into the workflow renders them visible.

4.3. Implications for planning

For practice, the framework turns a vague aspiration—making the green network more resilient—into a ranked, spatially explicit, and defensible plan of action. The high-confidence priorities, namely the large riparian and park cores, make the case for strict protection and for securing their water supply. The pinch-point corridors make the case for targeted measures—small parks, vegetated easements, permeable verges, or street-tree plantings—positioned where they add most to route redundancy. The stepping stones make the case for a dispersed strategy of many small, water-efficient patches in preference to a few large ones, an arrangement well matched to xeric and drought-tolerant planting and to coupling with stormwater capture. Because the resistance surface and dispersal threshold are explicit, the same workflow can be executed for different target organisms or planning scenarios, and because it is disturbance-aware, it can serve to test candidate interventions against simulated drought ahead of investment. In this respect the method reinforces the ecological security pattern tradition in planning (Yu, 1996) while broadening it with criteria of redundancy and robustness.

4.4. Relation to prior work

The framework rests directly on well-established traditions—morphological pattern analysis (Soille & Vogt, 2009; Vogt et al., 2007; Wickham et al., 2010), least-cost and security-pattern modelling (Knaapen et al., 1992; Adriaensen et al., 2003; Yu, 1996), and graph-based connectivity assessment (Pascual-Hortal & Saura, 2006; Saura & Pascual-Hortal, 2007; Saura & Rubio, 2010; Kong et al., 2010; Zetterberg et al., 2010)—and adds to them by drawing them together around an explicit resilience objective and a disturbance test. It complements circuit-theoretic connectivity modelling (McRae et al., 2008), which could replace or be joined with the MCR step wherever multi-path movement is the more appropriate assumption; the integration logic and the resilience indicators remain neutral with respect to that choice.

4.5. Limitations

Several caveats temper these results. First and foremost, the assessment presented here is an illustrative demonstration rather than a validated empirical study; its numerical outputs hinge on synthetic inputs and serve only to showcase the method, and applying it to a named city would require locally classified land cover, calibrated resistance values, and, ideally, independent validation against observed movement or genetic data. The resistance surface is the foremost source of uncertainty: lacking species-specific movement data, the values depend on expert judgement, and the corridor and connectivity outputs are sensitive to them—which is why the perturbation analysis and formal sensitivity testing matter. The results also depend on the MSPA edge width, the source-size threshold, the dispersal-distance parameter, and the composite weighting scheme; equal weighting was used here for transparency, but alternative schemes ought to be examined and reported. The analysis is two-dimensional and static, leaving out vegetation condition, seasonality, and the temporal dynamics of drought, and it relies on a generic, taxon-neutral dispersal profile instead of modelling particular species. Lastly, effective distances obtained from a cost surface are a model of movement, not a measurement of it.

4.6. Future directions

These limitations translate into a clear research agenda. Empirical application across a number of dryland cities, drawing on harmonised remote-sensing inputs, would test how general the structural and resilience patterns indicated here prove to be. Multi-temporal satellite data could power a dynamic version of the framework that follows resilience through wet and dry years and links it to hydrological and land-surface-temperature models, tying GI connectivity to water balance and the urban heat island. Swapping the single generic profile for multiple, taxon-specific resistance and dispersal parameters would generate multi-species resilience surfaces, while formal global sensitivity and uncertainty analysis would delimit the influence of parameter choices. Pairing the quantitative priorities with participatory planning would help convert them into workable, locally legitimate interventions.

5. CONCLUSION

Green infrastructure in arid cities is structurally sparse, fragmented, and acutely exposed to water stress, and its resilience cannot be inferred from any single connectivity metric. This study has formulated and demonstrated an integrated framework that links MSPA, MCR, and Conefor and makes resilience operational through redundancy, connectivity, and robustness against simulated disturbance. The combination amounts to more than the sum of its parts: morphological analysis discloses the structural scaffolding, least-cost modelling pinpoints the corridors and their bottlenecks, and graph-based indices rank elements by their systemic importance, while the composite score and disturbance scenarios set high-confidence priorities apart from the stepping stones that quietly supply redundancy. Applied with local data, the workflow gives planners a reproducible, spatially explicit, and disturbance-tested foundation for protecting hubs, strengthening fragile corridors, and distributing water-efficient green space where it does most to reinforce the network. Its value will be greatest once the framework is parameterised and validated for particular dryland cities and embedded within the wider water and climate-adaptation planning on which their green infrastructure ultimately depends.

REFERENCES

1. Adriaensen, F., Chardon, J. P., De Blust, G., Swinnen, E., Villalba, S., Gulinck, H., & Matthysen, E. (2003). The application of ‘least-cost’ modelling as a functional landscape model. Landscape and Urban Planning, 64(4), 233–247.
2. Benedict, M. A., & McMahon, E. T. (2006). Green Infrastructure: Linking Landscapes and Communities. Washington, DC: Island Press.
3. Folke, C. (2006). Resilience: The emergence of a perspective for social–ecological systems analyses. Global Environmental Change, 16(3), 253–267.
4. Forman, R. T. T. (1995). Land Mosaics: The Ecology of Landscapes and Regions. Cambridge: Cambridge University Press.
5. Grimm, N. B., Faeth, S. H., Golubiewski, N. E., Redman, C. L., Wu, J., Bai, X., & Briggs, J. M. (2008). Global change and the ecology of cities. Science, 319(5864), 756–760.
6. Holling, C. S. (1973). Resilience and stability of ecological systems. Annual Review of Ecology and Systematics, 4, 1–23.
7. Knaapen, J. P., Scheffer, M., & Tress, B. (1992). Estimating habitat isolation in landscape planning. Landscape and Urban Planning, 23(1), 1–16.
8. Kong, F., Yin, H., Nakagoshi, N., & Zong, Y. (2010). Urban green space network development for biodiversity conservation: Identification based on graph theory and gravity modeling. Landscape and Urban Planning, 95(1–2), 16–27.
9. McRae, B. H., Dickson, B. G., Keitt, T. H., & Shah, V. B. (2008). Using circuit theory to model connectivity in ecology, evolution, and conservation. Ecology, 89(10), 2712–2724.
10. Meerow, S., Newell, J. P., & Stults, M. (2016). Defining urban resilience: A review. Landscape and Urban Planning, 147, 38–49.
11. Pascual-Hortal, L., & Saura, S. (2006). Comparison and development of new graph-based landscape connectivity indices: Towards the prioritization of habitat patches and corridors for conservation. Landscape Ecology, 21(7), 959–967.
12. Pickett, S. T. A., Cadenasso, M. L., Grove, J. M., Nilon, C. H., Pouyat, R. V., Zipperer, W. C., & Costanza, R. (2001). Urban ecological systems: Linking terrestrial ecological, physical, and socioeconomic components of metropolitan areas. Annual Review of Ecology and Systematics, 32, 127–157.
13. Saura, S., & Pascual-Hortal, L. (2007). A new habitat availability index to integrate connectivity in landscape conservation planning: Comparison with existing indices and application to a case study. Landscape and Urban Planning, 83(2–3), 91–103.
14. Saura, S., & Rubio, L. (2010). A common currency for the different ways in which patches and links can contribute to habitat availability and connectivity in the landscape. Ecography, 33(3), 523–537.
15. Saura, S., & Torné, J. (2009). Conefor Sensinode 2.2: A software package for quantifying the importance of habitat patches for landscape connectivity. Environmental Modelling & Software, 24(1), 135–139.
16. Soille, P., & Vogt, P. (2009). Morphological segmentation of binary patterns. Pattern Recognition Letters, 30(4), 456–459.
17. Taylor, P. D., Fahrig, L., Henein, K., & Merriam, G. (1993). Connectivity is a vital element of landscape structure. Oikos, 68(3), 571–573.

18. Tzoulas, K., Korpela, K., Venn, S., Yli-Pelkonen, V., Kaźmierczak, A., Niemelä, J., & James, P. (2007). Promoting ecosystem and human health in urban areas using Green Infrastructure: A literature review. Landscape and Urban Planning, 81(3), 167–178.
19. Vogt, P., Riitters, K. H., Estreguil, C., Kozak, J., Wade, T. G., & Wickham, J. D. (2007). Mapping spatial patterns with morphological image processing. Landscape Ecology, 22(2), 171–177.
20. Walker, B., Holling, C. S., Carpenter, S. R., & Kinzig, A. (2004). Resilience, adaptability and transformability in social–ecological systems. Ecology and Society, 9(2), 5.
21. Wickham, J. D., Riitters, K. H., Wade, T. G., & Vogt, P. (2010). A national assessment of green infrastructure and change for the conterminous United States using morphological image processing. Landscape and Urban Planning, 94(3–4), 186–195.
22. Yu, K. (1996). Security patterns and surface model in landscape ecological planning. Landscape and Urban Planning, 36(1), 1–17.
23. Zetterberg, A., Mörtberg, U. M., & Balfors, B. (2010). Making graph theory operational for landscape ecological assessments, planning, and design. Landscape and Urban Planning, 95(4), 181–191.